

Carbonyl₄: A Sketch for Set-Increment Mixed Updates

Yikai Zhao
Peking University
Beijing, China
zyk@pku.edu.cn

Yuhan Wu
Peking University
Beijing, China
yuhan.wu@pku.edu.cn

Tong Yang
Peking University
Beijing, China
yangtong@pku.edu.cn

ABSTRACT

In the realm of data stream processing, the advent of SET-INCREMENT Mixed (SIM) data streams necessitates algorithms that efficiently handle both SET and INCREMENT operations. We present Carbonyl₄, an innovative algorithm designed specifically for SIM data streams, ensuring accuracy, unbiasedness, and adaptability. Carbonyl₄ introduces two pioneering techniques: the Balance Bucket for refined variance optimization, and the Cascading Overflow for maintaining precision amidst overflow scenarios. Our experiments across four diverse datasets establish Carbonyl₄'s supremacy over existing algorithms, particularly in terms of accuracy for item-level information retrieval and adaptability to fluctuating memory requirements. The versatility of Carbonyl₄ is further demonstrated through its dynamic memory shrinking capability, achieved via a re-sampling and a heuristic approach. The source codes of Carbonyl₄ are available at GitHub [1].

1 INTRODUCTION

Sketches are algorithms that succinctly approximate per-key information in data streams, enabling functions like point queries [2–4], subset queries [5–7], and Top-*K* queries [8–10]. They're applied in diverse areas, including databases [11–13], data mining [14–16], networking [17–19], and web services [20]. Unlike hash tables [21, 22], which record complete key-value pair information, sketches construct a highly accurate approximate representation of such pairs using sublinear space, offering a configurable balance between space efficiency and accuracy. For platforms with memory constraints, such as handheld devices, IoT networks, and high-performance ASICs, sketches are increasingly preferred due to their ability to deliver near-accurate measurements with tolerable error margins, thus providing satisfactory performance.

However, a notable shortcoming of sketches, when compared to their advantages in space efficiency and accuracy, is their limited support for certain types of updates in data streams. Unlike hash tables, sketches are not inherently designed to handle SET updates. Typically, each item in a data stream corresponds to a modification of a key's value. Both sketches and hash tables support INCREMENT updates ($e, "+ = ", v$), which increment the value associated with a

key e , akin to the SQL command:

$$\text{UPDATE table SET value} = \text{value} + v \text{ WHERE key} = e. \quad (1)$$

Yet, only hash tables facilitate SET updates ($e, " := ", v$), which completely replace the value for a key e , corresponding to the SQL statement:

$$\text{UPDATE table SET value} = v \text{ WHERE key} = e. \quad (2)$$

To illustrate, we present examples where data streams incorporate both INCREMENT and SET updates, a scenario we refer to as SET-INCREMENT Mixed (SIM) updates.

Sensor Data Collection: Sensors gather time-series data, with each sensor's ID acting as the key and its readings as the value. To optimize bandwidth, sensors switch between transmitting complete readings upon request (SET updates) and sending incremental changes at other times (INCREMENT updates), resulting in SIM updates [23, 24].

Batch Size Statistics: In data streams, a batch, or in networking terms, a flowlet, is defined by items with the same key e occurring within a certain time threshold T [25–27]. Tracking the size of these batches involves marking the first item as a reset point (SET updates) and subsequently counting additional items as they arrive (INCREMENT updates), leading to SIM updates.

Real-time Memory Monitoring: Monitoring memory usage in real-time for objects in live programs is crucial for developers. Tools like LLDB and JProfiler track memory by recognizing new or resized objects as SET updates and incremental memory additions as INCREMENT updates [28, 29]. This process, analogous to tracking keys in a data stream, also results in SIM updates.

Table 1: Comparison of update forms supported by different algorithms.

	Exact	Approximate
INCREMENT-Only	Hash Tables	Existing Sketches
SET-INCREMENT Mixed	Hash Tables	This Study

Table 1 delineates the capability of hash tables and sketches in managing distinct update forms. Hash tables can accurately process both INCREMENT-Only and SET-INCREMENT Mixed updates, while existing sketches are constrained to INCREMENT-Only updates with approximate results. Our contribution lies in the introduction of an innovative sketch tailored for SET-INCREMENT Mixed updates, which facilitates a more effective approximation of data streams with SIM updates. This development significantly enhances the memory efficiency and adaptability of applications, including the three exemplified cases, optimizing them for more streamlined and versatile deployment.

Permission to make digital or hard copies of all or part of this work for personal or classroom use is granted without fee provided that copies are not made or distributed for profit or commercial advantage and that copies bear this notice and the full citation on the first page. Copyrights for components of this work owned by others than ACM must be honored. Abstracting with credit is permitted. To copy otherwise, or republish, to post on servers or to redistribute to lists, requires prior specific permission and/or a fee. Request permissions from permissions@acm.org.

Conference'17, July 2017, Washington, DC, USA

© 2024 Association for Computing Machinery.

ACM ISBN 978-x-xxxx-xxxx-x/YY/MM... \$15.00

<https://doi.org/10.1145/nnnnnnn.nnnnnnn>

Before we introduce our solution, it is essential to understand why existing sketches have difficulty with SET updates. Sketches typically come in two varieties: counting sketches and key-value sketches. Counting sketches do not keep track of individual item keys, utilizing shared counters that permit hash collisions. Altering a counter to accommodate a SET value can inadvertently affect other items that collide in that counter, potentially breaching the error limits established by L_1 or L_2 norms, thus leading to significant errors. *Simply put, consider a task: recording the sum of values for all keys. If there are only INCREMENT updates, we could trivially use a single counter; however, if there are SET updates, we must record the value of each key.* Key-value sketches maintain keys and values for a subset of items within a bucket array, where items hashed to the same bucket vie for limited space using intricate replacement strategies. These strategies, however, are optimized for INCREMENT updates with minor and restricted increments, falling short in accuracy for SET updates that introduce a larger range of values.

In this work, we introduce Carbonyl₄, a sophisticated key-value sketch algorithm for data streams with Set-Increment mixed (SIM) updates, optimizing for limited memory. Carbonyl₄ adapts to the value distributions of SET and INCREMENT updates, supporting standard queries and offering enhanced accuracy across datasets. Its unbiased estimates ensure controlled errors, and its flexible design allows for dynamic memory management. We address two main challenges to achieve our objectives. The *Feasibility Challenge* involves managing SET updates to maintain algorithmic accuracy and function within L_1 or L_2 norm constraints. The *Dynamic Challenge* seeks to adapt to a wide range of SET update values, minimizing error propagation due to hash collisions.

In addressing the feasibility challenge, we extend the Probability Proportional to Size (PPS) sampling-based item competition approach, fundamental to existing unbiased sketches [5, 6]—termed *unbiased merging* in Section 2—from the positive integer domain \mathbb{N}^+ to the entire real number field \mathbb{R} . This extension lays the groundwork for the *Balance Bucket*, tailored to optimize local variance while maintaining unbiased estimates. Traditional replacement strategies in sketches [5, 9], which consistently merge any new item with the smallest existing value in the bucket, may be near-optimal for increment updates with fixed values but are not ideal for set updates where values can be substantially larger. Our *Balance Bucket* introduces a more nuanced approach, considering the size of the update value to determine the most advantageous merging strategy within the bucket, thereby providing an optimal solution for handling set updates.

To tackle the dynamic challenge, we implement an overflow mechanism that connects different *Balance Bucket* within a bucket array, assigning each item to a pair of buckets rather than just one. When processing an update, if the item values in the associated bucket are comparatively large, leading to potential significant errors during competition or replacement, we trigger an overflow. This process moves the item with the smallest value to another bucket that is also associated with that item. Termed as *Cascading Overflow*, this strategy unfolds in a cascading fashion, halting only upon activation of an in-built automatic adaptation protocol. Effectively, *Cascading Overflow* transitions the focus from minimizing local variance within individual buckets to achieving a broader,

near-global variance reduction by iterating through multiple buckets. This provides an expanded scope for accommodating updates with larger values. Unlike the feasibility challenge, which relies on theoretical analysis, the dynamic challenge is predominantly addressed through intricate algorithmic innovation.

Key Contributions: 1) Carbonyl₄ is introduced as the first algorithm designed for SET-INCREMENT mixed data streams, ensuring accuracy, unbiasedness, and flexibility. 2) Comprehensive experiments on various datasets confirm Carbonyl₄'s effectiveness for point, subset, and Top-K queries, outperforming existing approaches. 3) Advanced in-place shrinking algorithms are crafted to significantly boost Carbonyl₄'s flexibility without compromising on performance.

2 BACKGROUND

2.1 Problem Definition

We simplify our terminology by referring to data streams with Set-Increment mixed updates as Set-Increment mixed data streams (SIM streams). The formal definition is as follows:

DEFINITION 1. (SET-INCREMENT MIXED DATA STREAM) A Set-Increment mixed (SIM) data stream $\mathcal{S} = \{op_1, op_2, \dots, op_n\}$ consists of a sequence of updates op_i , each being either a set update $\langle e_i, " := ", v_i \rangle$ or an increment update $\langle e_i, " + = ", v_i \rangle$. Here, e_i denotes an item from the universal set \mathcal{U} , and v_i is a value from the set of real numbers \mathbb{R} . The true value of item $e \in \mathcal{U}$ after n updates is denoted as $R(e)$.

DEFINITION 2. (POINT QUERY) A point query over a SIM data stream \mathcal{S} , given an algorithm \mathcal{A} , requires \mathcal{A} to estimate the true value $R(e)$ of any item $e \in \mathcal{U}$, providing an approximation $Q(e)$.

(SUBSET QUERY) A subset query for a SIM data stream \mathcal{S} , under algorithm \mathcal{A} , requires an estimation of the cumulative true value $R(\mathcal{U}') = \sum_{e \in \mathcal{U}'} R(e)$ for any subset $\mathcal{U}' \subseteq \mathcal{U}$, denoted as $Q(\mathcal{U}')$.

(TOP-K QUERY) For a Top-K query on SIM data stream \mathcal{S} , algorithm \mathcal{A} is expected to identify K items with the highest true absolute values $|R(e)|$ and provide their corresponding estimates $Q(e)$.

DEFINITION 3. (L_1 NORM) The L_1 norm of a Set-Increment mixed data stream $\mathcal{S} = \{op_1, op_2, \dots, op_n\}$ is defined as the sum of the absolute values of the updates:

$$\|\mathcal{S}\|_1 = \sum_{i=1}^n |v_i|.$$

2.2 Related Work

We categorize the pertinent algorithms into three types: counting sketches, key-value sketches, and hash tables, assessing their adaptability to handle Set-Increment mixed (SIM) data streams with memory efficiency. Other related works also include [10, 13, 30–36], among others.

Counting Sketches. Counting sketches are tailored for increment-only data streams and share a common structure. Typically, they utilize a matrix of counters with d rows and w columns to log item values, associating each item with a counter in every row via d distinct hash functions. Popular counting sketches such as count-min (CM) sketch [2], Count sketch [4], conservative-update (CU) sketch [3], CMM sketch [37], CSM sketch [38], SALSA [39], among others [11, 40, 41], are differentiated by their counter update mechanisms.

For instance, CM sketch increments the hashed counters for each item directly across all rows, Count sketch adjusts the increment probabilistically based on the item's key, and CU sketch selectively increases only the smallest hashed counter, functioning exclusively with positive increments, denoted by $v_i > 0$. However, adapting counting sketches to accommodate Set-Increment mixed (SIM) data streams is infeasible, as they lack the mechanism to record individual item keys, rendering the identification of previous item values for set updates $\langle e, \text{" := ", } v \rangle$ unattainable.

Key-Value Sketches. Key-value sketches, primarily designed for increment-only data streams, function similarly to approximate hash tables by logging the keys and estimated values of a selection of items from the universal set \mathcal{U} . For instance, SpaceSaving [8] (SS) and Unbiased SpaceSaving [6] (USS) employ a modified heap structure of size K to keep track of the K items with the largest estimated values, handling increment updates where $v_i = 1$ to maintain $O(1)$ time complexity. The SpaceSaving[±] [42] algorithm extends this to manage $v_i = -1$. To accommodate set updates, SS, USS, and SS[±] would need to accept an update complexity of $O(\log K)$. Other key-value sketches, such as RAP [43], Elastic Sketch [9] (Elastic) and CocoSketch [5] (Coco), along with several others [7, 26, 44–46], replace the counters in a matrix with key-value pairs. Coco, an advanced unbiased sketch, provides fair estimates for each item but is limited to increment updates with non-negative values $v_i \geq 0$. Upon receiving an increment update $\langle e, \text{" + = ", } v \rangle$, Coco identifies the entry $\langle e', v' \rangle$ with the smallest value among the d hashed counterparts and merges them using the *unbiased merging* technique defined within the positive integer realm \mathbb{N}^+ as shown:

$$\text{MERGE}(\langle e, v \rangle, \langle e', v' \rangle) = \begin{cases} \langle e, v + v' \rangle & \text{with probability } \frac{v}{v+v'} \\ \langle e', v + v' \rangle & \text{with probability } \frac{v'}{v+v'} \end{cases}.$$

Altering Elastic or Coco to facilitate set updates seems straightforward—if an item e is pre-recorded, its estimated value is directly updated; otherwise, the set update is processed as an increment update. However, this approach can lead to substantial inaccuracies, as demonstrated in Section 6.

Hash Tables. A hash table requires $O((1 + \epsilon)n)$ slots to store the keys and corresponding values for n items, mapping each item to a slot or series of slots. Widely utilized hash tables, such as the Cuckoo hash table [21] and Hopscotch hashing [22], are designed to provide constant query time. In particular, the Cuckoo hash table uses two hash functions, h_1 and h_2 , to associate each item e with two slots $C[h_1(e)]$ and $C[h_2(e)]$. When inserting an item, if both slots are occupied, the table displaces one of the existing entries to an alternative slot, continuing this 'kicking' process until an empty slot is found or a preset kick count is exceeded. Hash tables are inherently capable of handling SIM data streams provided they have sufficient memory. Even with a load factor beyond 100%, the table can still process updates by discarding entries when the kick limit is reached, although this introduces significant errors, which we demonstrate in Section 6.

Association with Carbonyl₄: The Balance Bucket design draws from CocoSketch's data structure, and the Cascading Overflow concept takes cues from the Cuckoo hash table's collision strategy. Our

Carbonyl₄ algorithm, however, is uniquely tailored to the numerical dynamics of SIM data streams, detailing operations that extend beyond these initial inspirations.

3 CARBONYL₄ ALGORITHM

In this section, we delineate the utilization of a *Balance Bucket* for managing Set-Increment mixed data streams. The approach is crafted to ensure unbiased estimations and to minimize variance on a local scale. Subsequently, we present the *Cascading Overflow* technique, our novel contribution, aimed at extending variance minimization from a local to a near-global scope.

3.1 Balance Bucket

MERGE[±]: Extending to Real Numbers. To accommodate both set and increment updates for negative and non-integer values, we extend the concept of unbiased merging, $\text{MERGE}(\cdot, \cdot)$, from the domain of positive integers \mathbb{N}^+ to a more comprehensive operation, $\text{MERGE}^\pm(\cdot, \cdot)$, applicable over the real number field \mathbb{R} . This is accomplished by considering two entries $\langle e_1, v_1 \rangle$ and $\langle e_2, v_2 \rangle$ and merging them with a probability p calculated as:

$$p = \frac{|v_1|}{|v_1| + |v_2|}.$$

With probability p , MERGE^\pm returns the item e_1 with an updated value $\langle e_1, \text{sgn}(v_1)(|v_1| + |v_2|) \rangle$; with the complementary probability $1 - p$, it returns item e_2 with the updated value $\langle e_2, \text{sgn}(v_2)(|v_1| + |v_2|) \rangle$. The function $\text{sgn}(v)$ denotes the sign of a real number v . We introduce the concept of *merge cost* and assert its minimality for MERGE^\pm through the following theorem.

THEOREM 1. *The operator $\text{MERGE}^\pm(\langle e_1, v_1 \rangle, \langle e_2, v_2 \rangle)$ offers an unbiased estimate for the entries $\langle e_1, v_1 \rangle$ and $\langle e_2, v_2 \rangle$. The variance of this operator, termed the *merge cost*, is $2|v_1||v_2|$, which is proven to be optimal among all unbiased estimation operators.*

PROOF. The derivation of Theorem 1 follows directly from the arguments presented in Theorems 1 and 2 of reference [5]. \square

Data Structure: The Balance Bucket B consists of d entries, structured as depicted in Figure 1. Each entry, $B[i] = \langle B[i].K, B[i].V \rangle$, stores an item's key, $B[i].K$, and its corresponding estimated value, $B[i].V$, for the i -th item in the bucket.

Set Update: Handling an incoming set update $\langle e, \text{" := ", } v \rangle$ in bucket B unfolds in one of four scenarios:

Case 1: If item e is present in bucket B , with $B[i].K = e$, we directly overwrite the existing value with the new one, i.e., $B[i].V = v$.

Case 2: If item e is not in bucket B and there is at least one vacant entry, denoted by $B[i]$, we record e in this empty entry as $B[i] = \langle e, v \rangle$.

Case 3 (illustrated on the left side of Figure 1): If item e is not already in bucket B and all entries are occupied, we assume without loss of generality that

$$|B[1].V| \geq \dots \geq |B[d-1].V| \geq |B[d].V|,$$

and $|v| < |B[d-1].V|$. Under this assumption, we merge $\langle e, v \rangle$ with the entry possessing the smallest absolute value, $B[d]$, as:

$$B[d] = \text{MERGE}^\pm(\langle e, v \rangle, B[d])$$

with a merge cost of $2 \cdot |v| \cdot |B[d].V|$.

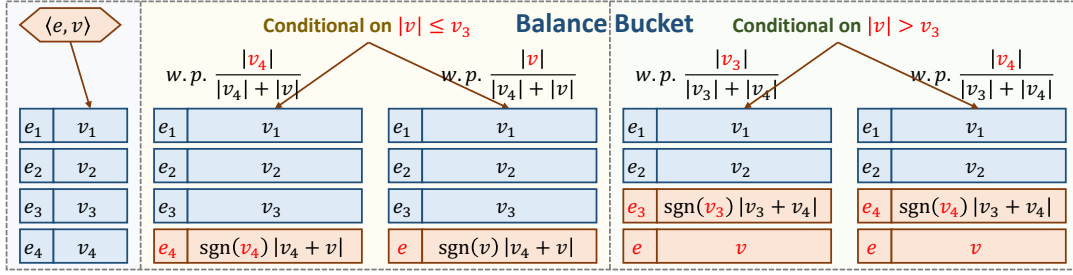


Figure 1: Balance Bucket. Bucket initial containing $d = 4$ entries $\langle e_1, v_1 \rangle, \dots, \langle e_4, v_4 \rangle$; the right side demonstrates four possible update scenarios when a new update $\langle e, v \rangle$ arrives: there are two possibilities when $|v| \leq |v_3|$, and two possibilities when $|v| > |v_3|$.

Case 4 (illustrated on the right side of Figure 1): If item e is not already in bucket B , all entries are filled, and $|v| \geq |B[d-1].V|$, we first merge the two entries with the smallest absolute values, $B[d-1]$ and $B[d]$, as:

$$B[d-1] = \text{MERGE}^\pm(B[d-1], B[d])$$

incurring a merge cost of $2 \cdot |B[d-1].V| \cdot |B[d].V|$. We then record the new update in $B[d]$ as $B[d] = \langle e, v \rangle$.

Increment Update: For incoming increment updates $\langle e, "+=", v \rangle$, the handling within bucket B can be categorized into the following cases:

Case 1: If item e is already recorded in bucket B , identified by $B[i].K = e$, we incrementally update the value: $B[i].V += v$.

Case 2, 3, and 4: Should item e be unrecorded in bucket B , the update is processed as $\langle e, "=", v \rangle$, adhering to the **Set Update** procedures outlined in Cases 2, 3, and 4.

The Rationale of Balance Bucket: In the context of Cocosketch, the value v associated with an increment update typically represents the size of a network packet, constrained by a maximum value (e.g., $v \leq 1500$), and is often substantially less than the least recorded value in the bucket, $|B[d].V|$, due to its monotonic increment. Conversely, in SIM data streams, both set and increment updates have the potential to decrease recorded values, resulting in scenarios where v could surpass the absolute value of the smallest recorded value, $|B[d].V|$, or even the second smallest, $|B[d-1].V|$. Consequently, discerning the optimal pairing for merging—by comparing $|v|$ with $|B[d-1].V|$ —is essential to achieve minimal merge cost and maintain the integrity of the Balance Bucket's data structure.

Point Query: To ascertain the estimated value of an item e , we scan each non-empty entry in the Balance Bucket B . If we find an entry corresponding to e (i.e., $B[i].K = e$), we return the recorded estimate $Q(e) = B[i].V$. If e is not found within the bucket, we conclude that $Q(e) = 0$.

THEOREM 2. (UNBIASEDNESS) For any item e within a universal set \mathcal{U} and subjected to a Set-Increment mixed (SIM) data stream S , let $R(e)$ denote the true value and $Q(e)$ the estimated value by the Balance Bucket. It holds that the expected value of the estimate is equal to the true value:

$$\mathbb{E}[Q(e)] = R(e).$$

THEOREM 3. (VARIANCE BOUND) Under the same setting as above, the expected sum of squared deviations between the estimated and

true values across all items in \mathcal{U} is bounded by:

$$\mathbb{E} \left[\sum_{e \in \mathcal{U}} (Q(e) - R(e))^2 \right] \leq \frac{2 \|S\|_1^2}{d}.$$

PROOF. Proofs for the above theorems are presented in detail in Section 5.1. \square

3.2 Carbonyl₄ with Cascading Overflow

While the Balance Bucket is effective, its capacity must be judiciously constrained to guarantee rapid and consistent update times. To address this, we introduce the fully-fledged Carbonyl₄ algorithm, which orchestrates multiple small Balance Bucket in tandem, each serving as a fundamental unit within the system.

Data Structure: The architecture of Carbonyl₄, as depicted in Figure 2, comprises w Balance Bucket B_1, \dots, B_w . Each Balance Bucket B_i houses d entries. The system employs two hash functions, $h_1(\cdot)$ and $h_2(\cdot)$, which uniformly map an item $e \in \mathcal{U}$ to one of the w buckets, with the stipulation that $h_1(e) \neq h_2(e)$ for any item e .

Set Update: When a set update $\langle e, "=", v \rangle$ arrives, Carbonyl₄ utilizes the hash functions to identify two corresponding Balance Bucket, $B_{h_1(e)}$ and $B_{h_2(e)}$, which we refer to as the hashed buckets for item e . If e is already present in either $B_{h_1(e)}$ or $B_{h_2(e)}$, we apply the overwriting strategy from Case 1 outlined in Section 3.1. Conversely, if e has not been recorded but an empty entry exists in either hashed bucket, we proceed as described in Case 2 from Section 3.1 to record the update. If neither condition is met, we select one hashed bucket at random and initiate a **Cascading Overflow** process, which seeks a near-globally optimal merge candidate within the system.

Cascading Overflow consists of two distinct phases: the searching stage and the kicking stage.

Searching Stage (illustrated on the upper portion of Figure 2): The searching stage initiates with the entry $\langle e, v \rangle$ and one of its hashed buckets, referenced as B_{idx} . We commence by setting a variable min_{global} to $+\infty$, representing the smallest merge cost encountered thus far. Under the assumption that

$$|B_{idx}[1].V| \geq \dots \geq |B_{idx}[d-1].V| \geq |B_{idx}[d].V|,$$

we compare the incoming value v with the penultimate smallest value $|B_{idx}[d-1].V|$ in the bucket. The objective is to identify a locally optimal merge within B_{idx} and to compute the corresponding

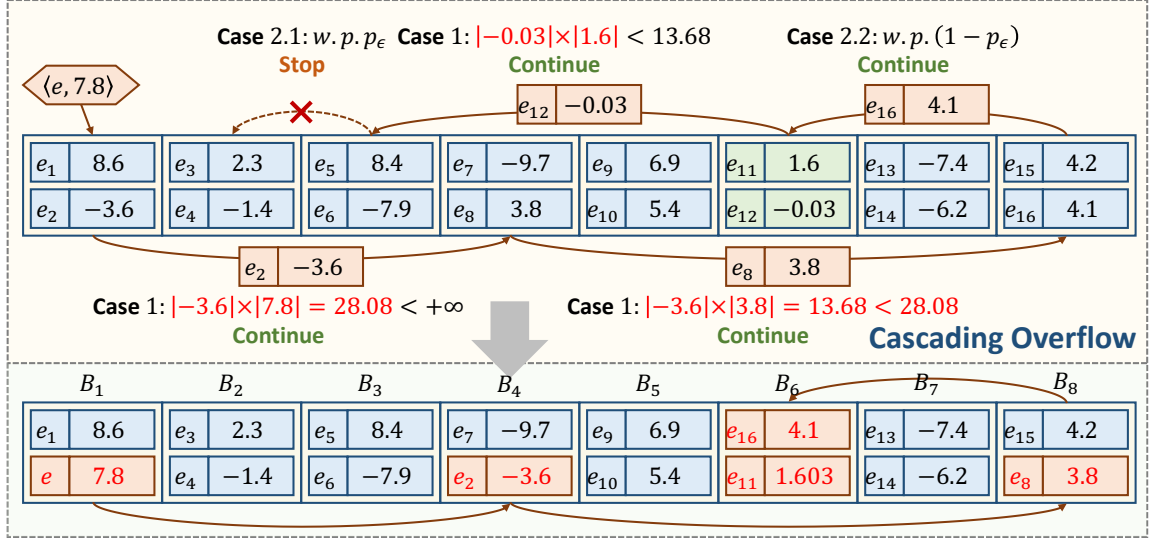


Figure 2: In a Cascading Overflow example: (a) Searching Stage: The process starts with the update $\langle e, 7.8 \rangle$ at bucket B_1 , with \min_{global} initially infinite. **Step 1:** $\min_{local} = 28.08$ prompts an update to \min_{global} , and the search moves to B_4 with $\langle e_2, -3.6 \rangle$. **Step 2:** \min_{global} becomes 13.68, and the search transitions to B_8 with $\langle e_8, 3.8 \rangle$. **Step 3:** With $\min_{local} \geq \min_{global}$, the search proceeds to B_6 with a chance of stopping. **Step 4:** A new low for \min_{global} at 0.123 leads to B_3 with $\langle e_{12}, -0.03 \rangle$. **Step 5:** The search may stop, with B_{opt} identified as B_6 . (b) Kicking Stage: Initiating at B_1 , the entry $\langle e, 7.8 \rangle$ causes a series of displacements across the buckets, ending with a merge in B_6 .

minimal merge cost, as detailed in lines 3-7 of the pseudo-code 1:

$$\min_{local} = \begin{cases} 2 \cdot |v| \cdot |B_{idx}[d] \cdot V| & \text{if } |v| \leq |B_{idx}[d-1] \cdot V|, \\ 2 \cdot |B_{idx}[d] \cdot V| \cdot |B_{idx}[d-1] \cdot V| & \text{if } |v| > |B_{idx}[d-1] \cdot V|. \end{cases}$$

- **Case 1:** If \min_{local} is less than the global minimum \min_{global} , we update $\min_{global} = \min_{local}$ as per lines 8-10 in pseudo-code 1. The smallest entry in B_{idx} , $B_{idx}[d]$, is then treated as the insertion candidate, and the search proceeds to the alternate hashed bucket of $B_{idx}[d] \cdot K$, following lines 14-17 in the pseudo-code.
- **Case 2:** If $\min_{local} \geq \min_{global}$, we have two subcases:
 - **Case 2.1:** The searching stage halts with probability p_ϵ , detailed in lines 11-13 of the pseudo-code.
 - **Case 2.2:** The search continues with the remaining probability, echoing the procedure in Case 1, as outlined in lines 14-17 of the pseudo-code.

The number of search steps may be capped at a maximum value M to constrain the process.

Kicking Stage (illustrated on the lower part of Figure 2): Upon concluding the searching stage, the kicking stage commences with the entry $\langle e, v \rangle$ and its associated buckets B_{idx} . We operate under the assumption that the absolute values within B_{idx} are ordered as

$$|B_{idx}[1] \cdot V| \geq \dots \geq |B_{idx}[d-1] \cdot V| \geq |B_{idx}[d] \cdot V|.$$

The entry $B_{idx}[d]$ is replaced by $\langle e, v \rangle$ (i.e., $B_{idx}[d] = \langle e, v \rangle$), and the displaced $B_{idx}[d]$ becomes the new candidate for insertion, perpetuating the kick through its alternate hashed bucket. This process iterates until a bucket B_{opt} is located, where the local minimum

merge cost aligns with the near-global minimum, \min_{global} , identified in the searching stage. The set update mechanics of the Balance Bucket, as delineated in Section 3.1, are then executed within B_{opt} , concluding the kicking phase. Notably, should an empty entry be encountered during the search, \min_{global} becomes zero, and the kicking phase will cease at that juncture, negating further action.

The Rationale of Cascading Overflow: In a SIM data stream, when the incoming value $|v|$ and the penultimate smallest value $|B[d-1] \cdot V|$ within a hashed bucket B substantially exceed the mean of the least absolute values recorded across buckets, merging $B[d]$ with either $\langle e, v \rangle$ or $B[d-1]$ becomes suboptimal. Cascading Overflow's strategy is to identify a near-globally optimal merge within the constraints of the predetermined time complexity. This approach is adaptive, with extensive searching when the initial merge cost is high, and abbreviated steps when the initial cost is already minimal.

THEOREM 4. (EXPECTED NUMBER OF SEARCHING STEPS) Consider a Set-Increment mixed (SIM) data stream \mathcal{S} and Carbonyl₄ parameterized with $p_\epsilon = \frac{\epsilon}{(1-\sqrt{\epsilon})^2}$. The expected number of steps in the searching stage of the Cascading Overflow process is bounded by $O\left(\frac{1}{\epsilon}\right)$.

PROOF. The detailed proof is elaborated in Section 5.2. \square

Increment Update: When processing an increment update $\langle e, "+", v \rangle$, the two hash functions determine the corresponding Balance Bucket $B[h_1(e)]$ and $B[h_2(e)]$. If e is already present in either bucket, we increment the stored value as per the method described in Case 1 of Section 3.1. If e is not recorded in either bucket, the update

Algorithm 1: Routine for the searching stage.

```

1 Func Searching( $idx, \langle e, v \rangle, min_{global}$ ):
2   ▶ Assume  $B_{idx}$  entries are sorted.
3   if  $|v| \leq |B_{idx}[d-1].V|$  then
4      $min_{local} = |v| \times |B_{idx}[d].V|$ ;
5   else
6      $min_{local} = |B_{idx}[d].V| \times |B_{idx}[d-1].V|$ ;
7   ▶ Compute local optimal merge.
8   if  $min_{local} < min_{global}$  then
9      $min_{global} \leftarrow min_{local}$ ;
10    ▶ Update for better merge.
11  else if  $r \in Uniform(0,1) \leq p_\epsilon$  then
12    ▶ Stop with chance  $p_\epsilon$ .
13    return;
14   $idx \leftarrow Another\_Index(B[d].K, idx)$ ;
15   $\langle e, v \rangle \leftarrow B[d]$ ;
16  ▶ Continue with next bucket.
17  Searching( $idx, \langle e, v \rangle, min_{global}$ );

```

Algorithm 2: Routine for the kicking stage.

```

1 Func Kicking( $idx, \langle e, v \rangle, min_{global}$ ):
2   ▶ Assume  $B_{idx}$  entries are sorted.
3   if  $|v| \cdot |B_{idx}[d].V| = min_{global}$  then
4      $B_{idx}[d] \leftarrow MERGE^\pm(\langle e, v \rangle, B_{idx}[d])$ ;
5     ▶ Merge and end if local equals global.
6   else if  $|B_{idx}[d].V| \cdot |B_{idx}[d-1].V| = min_{global}$  then
7      $B_{idx}[d-1] \leftarrow MERGE^\pm(B_{idx}[d], B_{idx}[d-1])$ ;
8      $B_{idx}[d] \leftarrow \langle e, v \rangle$ ;
9     ▶ Merge and end if local equals global.
10  else
11     $idx \leftarrow Another\_Index(B[d].K, idx)$ ;
12    Swap( $\langle e, v \rangle, \langle B[d].K, B[d].V \rangle$ );
13    ▶ Kick and continue with next bucket.
14    Kicking( $idx, \langle e, v \rangle, min_{global}$ );

```

is handled as a set update $\langle e, \cdot := v \rangle$, following the complete **Set Update** procedure.

Point Query: To retrieve the estimated value for an item e , we inspect all entries in the buckets $B_{h_1(e)}$ and $B_{h_2(e)}$. If e is found (i.e., $B_{h_i(e)}[j].K = e$), the estimated value is given by $B_{h_i(e)}[j].V$; if not, the estimated value defaults to zero.

Subset Query: The estimated sum for a subset \mathcal{U}' within the universal set \mathcal{U} is computed by summing the estimated values of the subset's items across all buckets in $Carbonyl_4$: $\sum_{i=1}^w \sum_{B_i[j].K \in \mathcal{U}'} B_i[j].V$.

Top-K Query: To identify the K items with the highest absolute estimated values, we traverse every entry in all w buckets of $Carbonyl_4$ and return the K entries with the largest absolute values.

THEOREM 5. (UNBIASEDNESS) Given a SIM data stream \mathcal{S} and a universal set \mathcal{U} , for any subset $\mathcal{U}' \subseteq \mathcal{U}$, the $Carbonyl_4$ provides an unbiased estimation of the sum. That is, if $R(e)$ is the true value and $Q(e)$ is the estimated value provided by $Carbonyl_4$ for any item $e \in \mathcal{U}$, then:

$$\mathbb{E} \left[\sum_{e \in \mathcal{U}'} Q(e) \right] = \sum_{e \in \mathcal{U}'} R(e).$$

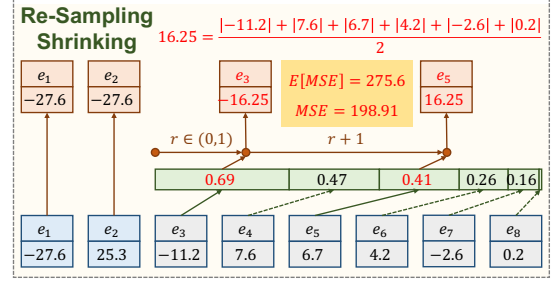


Figure 3: Re-Sampling shrinking. Initially, there are a total of 8 entries (in blue) from two buckets, and after shrinking, there remain 4 entries (in orange) placed in one bucket.

PROOF. The comprehensive proof is detailed in Section 5.3. \square

4 FLEXIBILITY OF CARBONYL₄

Flexibility is crucial for approximate algorithms, allowing for dynamic memory allocation to balance between precision and resource availability. This section contrasts the conventional re-build approach for memory adjustments with two novel in-place shrinking algorithms designed for $Carbonyl_4$. These algorithms significantly expedite the shrinking process, improving speed by more than 20-fold. One algorithm aims to surpass the average accuracy of re-build with a near-optimal re-sampling strategy, while the other is specifically tailored to enhance performance for Top- K queries.

4.1 Re-Build based Expanding and Shrinking

Adjusting the size of $Carbonyl_4$ involves transforming an existing sketch C with w buckets into a revised sketch C' with w' buckets. When the ratio $\frac{w}{w'}$ is less than a certain threshold α , which is below the standard load factor for cuckoo hash tables, the new sketch C' is populated by treating it as a cuckoo hash table with a stopping probability p_ϵ set to zero. This means we can directly insert entries from C into C' without interruption. Conversely, if the ratio $\frac{w}{w'}$ meets or exceeds α , the stopping probability p_ϵ must be determined based on a complexity level that is deemed acceptable for the operation, before transferring entries from C to C' .

4.2 Re-Sampling based In-place Shrinking

While re-build based resizing offers high flexibility and accuracy for adjusting $Carbonyl_4$'s memory footprint, it can be time-consuming. This is especially problematic for shrinking, which is often necessitated by the immediate need to reallocate resources to more critical tasks. For scenarios requiring a reduction of $Carbonyl_4$'s memory usage to half, an expedient method is to merge corresponding pairs of buckets, B_k and $B_{k+\frac{w}{2}}$, directly into B_k . This in-place operation not only executes swiftly but also requires only a simple adjustment to the hash functions, setting $h'_i(e) = h_i(e) \% w'$. This section introduces an optimal re-sampling strategy specifically designed for the efficient merging of bucket pairs when reducing the $Carbonyl_4$ size.

Re-Sampling Shrinking: As depicted in Figure 3, given two full buckets B_k and $B_{k+\frac{w}{2}}$, our task is to downsize by selecting d entries

from the combined $2d$. The entries are sorted by their absolute values in descending order, yielding the sequence $\langle e_1, v_1 \rangle, \dots, \langle e_d, v_d \rangle$. We then assess each entry beginning with the largest, against the criterion:

$$(d - i + 1) \times \frac{|v_i|}{\sum_{j=i}^{2d} |v_j|} \geq 1.$$

Entries meeting this condition are placed directly into B_k . If not, it implies for all $j \geq i$, the probability $p_j = \frac{(d-i+1)|v_j|}{\sum_{l=i}^{2d} |v_l|}$ is less than one. Therefore, we need to sample $(d - i + 1)$ entries based on their probabilities from the remaining set.

Independent sampling might not yield precisely $(d - i + 1)$ entries, necessitating a non-independent approach. We set auxiliary variables $r_{i-1} = 0$ and $r_j = \sum_{l=i}^j p_l$ for all $j \geq i$, then draw a random number r uniformly between 0 and 1. For integers z from 0 to $(d - i)$, we identify j such that $r_{j-1} \leq r + z < r_j$ and select $\langle e_j, v_j \rangle$ for unbiased re-sampling, placing $\langle e_j, \text{sgn}(v_j) \frac{\sum_{l=i}^{2d} |v_l|}{d-i+1} \rangle$ into B_k . The time complexity for re-sampling each pair of buckets is $O(d \log(d))$, summing to $O(wd \log(d))$ for the entire Carbonyl₄.

THEOREM 6. (OPTIMALITY) *The re-sampling method described guarantees unbiased selection from two combined buckets B_k and $B_{k+\frac{w}{2}}$, and achieves the least total variance among all unbiased sampling algorithms.*

PROOF. Section 1.4 of reference [47] introduces IPPS (Inclusion Probabilities Proportional to Size) sampling as the optimal variance-minimizing algorithm. Our re-sampling technique is an application of IPPS with a fixed sample size, following the methodology in Section 2.1 of reference [48]. \square

4.3 Heuristic based In-place Shrinking

Minimizing total variance through re-sampling is effective for merging buckets B_k and $B_{k+\frac{w}{2}}$, but certain applications, particularly those prioritizing Top-K query accuracy, may require preserving the precision of entries with larger absolute values while maintaining unbiasedness. Addressing this, we introduce a heuristic bucket merging approach tailored to optimize Top-K query performance post-shrinking.

Heuristic Shrinking: In situations where buckets B_k and $B_{k+\frac{w}{2}}$ lack empty entries, merging $2d$ entries into d necessitates d merge operations, as depicted in Figure 4. The heuristic method prioritizes accuracy for larger absolute values by consistently merging the two smallest entries in each step. Employing a min-heap to facilitate this process, the complexity of each merge is $O(\log(d))$, culminating in a total complexity of $O(wd \log(d))$ for the entire Carbonyl₄.

5 MATHEMATICAL ANALYSIS

This section is dedicated to substantiating key properties of Carbonyl₄ through rigorous proofs. We will focus on establishing the unbiased nature and variance constraints of the Balance Bucket, as articulated in Theorem 2 and Theorem 3 in Subsection 5.1. Additionally, we delve into the computational efficiency of the Cascading Overflow process as detailed in Theorem 4 within Subsection 5.2, and confirm the unbiasedness of subset queries in Carbonyl₄, outlined in Theorem 5, which is further explored in Subsection 5.3.

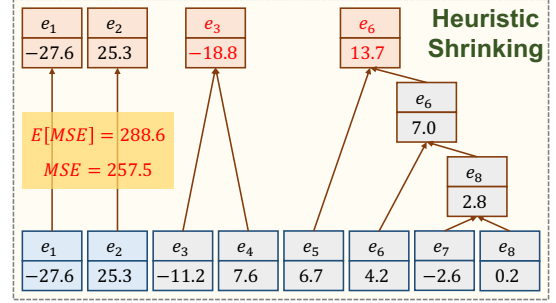


Figure 4: Heuristic shrinking. Initially, there are a total of 8 entries (in blue) from two buckets, and after shrinking, there remain 4 entries (in orange) placed in one bucket.

5.1 Analysis of Balance Bucket

DEFINITION 4. *Given a Set-Increment mixed (SIM) data stream $S = \{op_1, \dots, op_n\}$ and a Balance Bucket B , let $Q(e, i)$ be the estimated value of item e by the Balance Bucket after the i -th update, and $R(e, i)$ be the true value of item e .*

Proof of Unbiasedness (Theorem 2):

PROOF. We begin by assuming $\mathbb{E}[Q(e, i-1)] = R(e, i-1)$ and seek to demonstrate that $\mathbb{E}[Q(e, i)] = R(e, i)$ follows.

When $op_i = \langle e_i, "=" \rangle$ with $e_i = e$, we have $R(e, i) = v_i$. In the event of case 1 (refer to Section 3.1), $Q(e, i)$ is set to v_i . In cases 2 and 4, e is assigned an entry, making $Q(e, i)$ equal to v_i . In case 3, merging $\langle e, v \rangle$ with $B[d]$ results in:

$$\mathbb{E}[Q(e, i)] = \frac{|v_i|}{|v_i| + |B[d].V|} \cdot \text{sgn}(v_i)(|v_i| + |B[d].V|) = v_i,$$

establishing that $\mathbb{E}[Q(e, i)] = R(e, i)$.

For an increment update $op_i = \langle e_i, "+" \rangle$ where $e_i = e$, $R(e, i)$ is updated to $R(e, i-1) + v_i$. In case 1, $Q(e, i)$ becomes $Q(e, i-1) + v_i$. In cases 2 and 4, where $Q(e, i-1) = 0$, e receives an entry, and thus $Q(e, i) = v_i$. In case 3, where $Q(e, i-1) = 0$, merging is necessary, and so $\mathbb{E}[Q(e, i)] = v_i$. This confirms that $\mathbb{E}[Q(e, i)] = \mathbb{E}[Q(e, i-1)] + v_i = R(e, i)$.

For all other updates $op_i = \langle e_i, "*" \rangle$ with $e_i \neq e$, $R(e, i)$ remains $R(e, i-1)$. Cases 1 and 2 ensure $Q(e, i) = Q(e, i-1)$. In cases 3 and 4, if e is present and must merge, then $\mathbb{E}[Q(e, i)] = Q(e, i-1)$; otherwise, $Q(e, i)$ remains $Q(e, i-1)$. Thus, we conclude that $\mathbb{E}[Q(e, i)] = \mathbb{E}[Q(e, i-1)] = R(e, i)$.

Since $\mathbb{E}[Q(e, 0)] = R(e, 0) = 0$, and the inductive hypothesis holds for all i , it follows that $\mathbb{E}[Q(e, n)] = R(e, n)$, hence $\mathbb{E}[Q(e)] = R(e)$. \square

Proof of Variance Bound (Theorem 3):

PROOF. Consider the incremental variance Δ_i expressed by:

$$\begin{aligned} \Delta_i &= \mathbb{E} \left[\sum_{e \in U} (Q(e, i) - R(e, i))^2 \right] \\ &\quad - \mathbb{E} \left[\sum_{e \in U} (Q(e, i-1) - R(e, i-1))^2 \right] \\ &= \mathbb{E} \left[\sum_{e \in U} (Q(e, i) - R(e, i))^2 - (Q(e, i-1) - R(e, i-1))^2 \right], \end{aligned}$$

pertaining to items where either $Q(e, i) \neq Q(e, i-1)$ or $R(e, i) \neq R(e, i-1)$.

In the scenario where $op_i = \langle e_i, " := ", v_i \rangle$, and specifically for case 1 and case 2, we have:

$$(Q(e_i, i) - R(e_i, i))^2 - (Q(e_i, i-1) - R(e_i, i-1))^2 \leq 0;$$

For case 3, the merging of entry $\langle e_i, v_i \rangle$ with $B[d]$ leads to:

$$\begin{aligned} &\mathbb{E} \left[\begin{aligned} &(Q(e_i, i) - R(e_i, i))^2 \\ &+(Q(B[d].K, i) - R(B[d].K, i))^2 \\ &-(Q(e_i, i-1) - R(e_i, i-1))^2 \\ &-(Q(B[d].K, i-1) - R(B[d].K, i-1))^2 \end{aligned} \right] \\ &= (|v_i| + |B[d].V|)^2 - |v_i|^2 - |B[d].V|^2 - R(e_i, i-1)^2 \\ &= 2|v_i||B[d].V| - R(e_i, i-1)^2 \leq 2|v_i||B[d].V|. \end{aligned}$$

When dealing with the insertion of entry $B[d-1]$ alongside $B[d]$ in case 4, the variance increases by:

$$\begin{aligned} &\mathbb{E} \left[\begin{aligned} &(Q(B[d-1].K, i) - R(B[d-1].K, i))^2 \\ &+(Q(B[d].K, i) - R(B[d].K, i))^2 \\ &-(Q(B[d-1].K, i-1) - R(B[d-1].K, i-1))^2 \\ &-(Q(B[d].K, i-1) - R(B[d].K, i-1))^2 \end{aligned} \right] \\ &= (|B[d-1].V| + |B[d].V|)^2 - |B[d-1].V|^2 - |B[d].V|^2 \\ &= 2|B[d-1].V||B[d].V| \leq 2|v_i||B[d].V|. \end{aligned}$$

Therefore, each $\Delta_i \leq 2|v_i||B[d].V|$.

Applying similar logic to increment updates $op_i = \langle e_i, "+", v_i \rangle$, we also deduce that $\Delta_i \leq 2|v_i||B[d].V|$.

Acknowledging that

$$|B[d].V| \leq \frac{\sum_{i=1}^d |B[i].V|}{d} \leq \frac{\|\mathcal{S}\|_1}{d},$$

it follows that $\Delta_i \leq 2|v_i| \frac{\|\mathcal{S}\|_1}{d}$. Aggregating all Δ_i values, we obtain:

$$\begin{aligned} &\mathbb{E} \left[\sum_{e \in U} (Q(e) - R(e))^2 \right] \leq \sum_{i=1}^n \Delta_i \\ &\leq \left(\sum_{i=1}^n 2|v_i| \right) \frac{\|\mathcal{S}\|_1}{d} = \frac{2\|\mathcal{S}\|_1^2}{d}. \end{aligned}$$

□

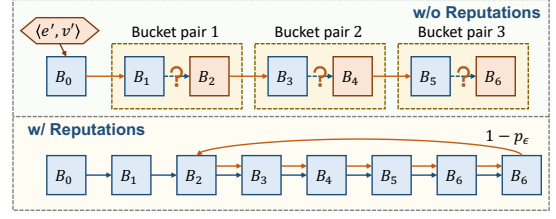


Figure 5: Illustration of Time Complexity.

5.2 Analysis of Cascading Overflow

Proof of Time Complexity (Theorem 4):

PROOF. Assume the searching stage begins at bucket B_0 , with successive buckets denoted as B_1, B_2, \dots . We initially address the case without bucket duplication along the path. Illustrated in Figure 5, we group buckets in consecutive pairs, thereby considering the local optimal merge cost min_{local} within bucket B_{2k} and B_{2k+2} as independent random variables. We simplify the stopping condition, only contemplating the cessation of the searching stage between buckets B_{2k-1} and B_{2k} , and not between B_{2k} and B_{2k+1} .

With this setup, the searching stage is segmented into two phases: the first seeks a sufficiently small min_{local} as the near-global minimal merge cost min_{global} ; the second estimates the expected number of steps to halt the process. To find a bucket B^* with min_{local} smaller than that of ϕw buckets, the expected number of steps required is

$$\begin{aligned} &\mathbb{E}[\text{number of steps in phase 1}] \\ &\leq \sum_{k=1}^{w/2} 2k(1-\phi)^{k-1}\phi \leq \frac{2}{\phi}. \end{aligned}$$

Upon updating the near-global optimal merge cost min_{global} to min_{local} of B^* , the stopping probability at each bucket B_{2k} becomes

$$\Pr[\text{stop probability}] = (1-\phi)p_\epsilon.$$

The expected step count to stop in phase two is then

$$\begin{aligned} &\mathbb{E}[\text{number of steps in phase 2}] \\ &\leq \sum_{k=1}^{w/2} 2k(1-(1-\phi)p_\epsilon)^{k-1}((1-\phi)p_\epsilon) \leq \frac{2}{(1-\phi)p_\epsilon}. \end{aligned}$$

For any $\phi \in (0, 1)$, the expected step count in the searching stage is

$$\begin{aligned} &\mathbb{E}[\text{number of steps in searching stage}] \\ &\leq \min \left(\frac{2}{\phi} + \frac{2}{(1-\phi)p_\epsilon} \right) = 2 \frac{(\sqrt{p_\epsilon} + 1)^2}{p_\epsilon}. \end{aligned}$$

Substituting $p_\epsilon = \frac{\epsilon}{(1-\sqrt{\epsilon})^2}$ yields

$$\begin{aligned} &\mathbb{E}[\text{number of steps in searching stage}] \\ &\leq 2 \frac{\left(\sqrt{\frac{\epsilon}{(1-\sqrt{\epsilon})^2}} + 1 \right)^2}{\frac{\epsilon}{(1-\sqrt{\epsilon})^2}} = \frac{2}{\epsilon} = O\left(\frac{1}{\epsilon}\right). \end{aligned}$$

Accounting for duplicate buckets on the search path, as depicted in Figure 5, the search loops upon encountering the first repeat bucket. Given that there is no item displacement in this stage, and

that \min_{global} ceases to update, the search is likely to conclude sooner than in the non-duplicate scenario, maintaining the expected step count at $O\left(\frac{1}{\epsilon}\right)$. \square

5.3 Analysis of Carbonyl₄

The proof of unbiasedness for Carbonyl₄ is similar to the proof of unbiasedness for Balance Bucket, but it additionally considers the effects of Cascading Overflow.

Proof of Unbiasedness (Theorem 5):

PROOF. Theorem 5's proof closely follows the rationale of Theorem 2, where we establish that $\mathbb{E}[Q(e, i - 1)] = R(e, i - 1)$ implies $\mathbb{E}[Q(e, i)] = R(e, i)$.

For a set update $op_i = \langle e_i, " := ", v_i \rangle$ with $e_i = e$, we have $R(e, i) = v_i$. In situations where item e is recorded in either bucket $B_{h_1(e)}$ or $B_{h_2(e)}$, or when there are empty slots in these buckets, or if the searching stage identifies another bucket as B_{opt} , it follows that $Q(e, i) = v_i$. If the searching stage designates $B_{h_1(e)}$ or $B_{h_2(e)}$ as B_{opt} , the analysis in cases 3 and 4 of Theorem 2 ensures $\mathbb{E}[Q(e, i)] = v_i$. Hence, $\mathbb{E}[Q(e, i)] = R(e, i)$ holds.

For an increment update $op_i = \langle e_i, "+ = ", v_i \rangle$ with $e_i = e$, $R(e, i) = R(e, i - 1) + v_i$. If item e is recorded or if a vacancy exists in $B_{h_1(e)}$ or $B_{h_2(e)}$, or if B_{opt} is determined during the searching stage, then $Q(e, i) = Q(e, i - 1) + v_i$ is maintained. Following the analysis in Theorem 2 for cases 3 and 4, if $B_{h_1(e)}$ or $B_{h_2(e)}$ becomes B_{opt} , we also deduce $\mathbb{E}[Q(e, i)] = Q(e, i - 1) + v_i$. Consequently, $\mathbb{E}[Q(e, i)] = \mathbb{E}[Q(e, i - 1)] + v_i = R(e, i)$.

In instances where $op_i = \langle e_i, *, v_i \rangle$ and $e_i \neq e$, $R(e, i)$ stays consistent with $R(e, i - 1)$. If item e is absent from B_{opt} in Cascading Overflow, then $Q(e, i) = Q(e, i - 1)$ is valid. Otherwise, according to Theorem 2, we infer $\mathbb{E}[Q(e, i)] = Q(e, i - 1)$. Thus, $\mathbb{E}[Q(e, i)] = \mathbb{E}[Q(e, i - 1)] = R(e, i)$.

Given that $\mathbb{E}[Q(e, 0)] = R(e, 0) = 0$, and by induction, for $i = n$, we conclude $\mathbb{E}[Q(e, n)] = R(e, n)$, that is, $\mathbb{E}[Q(e)] = R(e)$. The linearity of expectation allows us to express

$$\mathbb{E}\left[\sum_{e \in \mathcal{U}'} Q(e)\right] = \sum_{e \in \mathcal{U}'} \mathbb{E}[Q(e)] = \sum_{e \in \mathcal{U}'} R(e).$$

\square

6 EXPERIMENTAL RESULTS

We evaluate Carbonyl₄'s performance from the following key aspects.

- Accuracy of approximately recording the entire data stream (§6.2).
- Identification and approximation of Top- K items in a compact memory space (§6.3).
- Influence of Carbonyl₄'s parameters and data stream traits on performance and complexity (§6.4).
- Efficiency of Carbonyl₄'s shrinking algorithm versus full reconstruction (§6.5).

This concise exploration confirms Carbonyl₄'s robustness and adaptability.

6.1 Experiment Setup

Dataset:

- *The CAIDA dataset* [49] includes anonymized network trace data over one hour. A 4-byte source IP serves as the key, coupled with a 2-byte packet size as the value. A new flowlet is distinguished if the time between packets exceeds 1ms, indicated by a $:=$ operation; otherwise, a $+ =$. For analysis, we focus on the first 10M items.
- *The Synthetic dataset* is generated with 4-byte keys according to a Zipfian distribution [50] with $\alpha = 0.9$, replicating real-world long-tail distributions. Half of the dataset's items are associated with $:=$ operations with values derived from an EXP(10) distribution, and the other half with $+ =$ operations with values from a $N(0, 10)$ distribution. For analysis, we focus on the first 10M items.
- *The Webpage dataset* [51] records sequences of word occurrences in web documents, using a 4-byte word code as the key and frequency 1 as the value. A new burst is recognized when words are separated by more than 1000 others, signified by a $:=$ operation; otherwise, a $+ =$. For analysis, we focus on the first 10M items.
- *The Criteo dataset* [52] details advertisement features and feedback spanning 24 days, utilizing a 4-byte categorical feature as the key and an average of 13 numerical features as the value. Operations are equally divided between $:=$ and $+ =$. For analysis, we focus on the first 10M items.

Metrics: The assessment of Carbonyl₄ employs the following metrics:

- *ARE (Average Relative Error):* Defined as the mean of the relative errors for each item key, it is calculated as $\frac{\sum_{e \in \mathcal{U}} \frac{|R(e) - Q(e)|}{|R(e)|}}{|\mathcal{U}|}$, where $R(e)$ is the actual value of item e , and $Q(e)$ is the estimated value.
- *AAE (Average Absolute Error):* This metric represents the average of the absolute differences between true and estimated values for all items, defined as $\frac{\sum_{e \in \mathcal{U}} |R(e) - Q(e)|}{|\mathcal{U}|}$.
- *MSE (Mean Squared Error):* This measures the mean of the squared differences, formulated as $\frac{\sum_{e \in \mathcal{U}} (R(e) - Q(e))^2}{|\mathcal{U}|}$.
- *Recall Rate:* Employed to evaluate the precision in identifying Top- K items, the recall rate is calculated as the proportion of accurately identified Top- K items in the estimated set $\tilde{\mathcal{T}}$ compared to the true set \mathcal{T} , given by $\frac{|\tilde{\mathcal{T}} \cap \mathcal{T}|}{|\tilde{\mathcal{T}}|}$.
- *Throughput (Mops):* A metric assessing the number of insertions or queries an algorithm can perform in a unit of time (1 second).

These metrics facilitate a thorough evaluation of Carbonyl₄'s performance across different use cases and are crucial for substantiating its superiority over competing algorithms.

Default Setting: We implement Carbonyl₄ alongside comparison algorithms—Cuckoo hash [21] (Cuckoo), Unbiased SpaceSaving [6] with SET (USS*), CocoSketch [5] with SET (Coco*), and Elastic Sketch [9] (Elastic) in C++. All associated code is openly available on Github [1]. Our experiments are conducted on i9-10980XE CPUs under Linux, with a baseline frequency of 4GHz. For Carbonyl₄, Cuckoo, Coco*, and Elastic, the parameter d is set to 4. In Carbonyl₄, M is 10, and p_ϵ is 0.1. For SET updates, Coco*, USS*, and Elastic overwrite the existing value with a new value if the key is already recorded, or treat it as an INCREMENT update if the key is not recorded. Elastic only uses the heavy part. USS* is emulated with a heap and dictionary, adding four pointers per key-value pair to estimate memory overhead. For Cuckoo, we discard items that

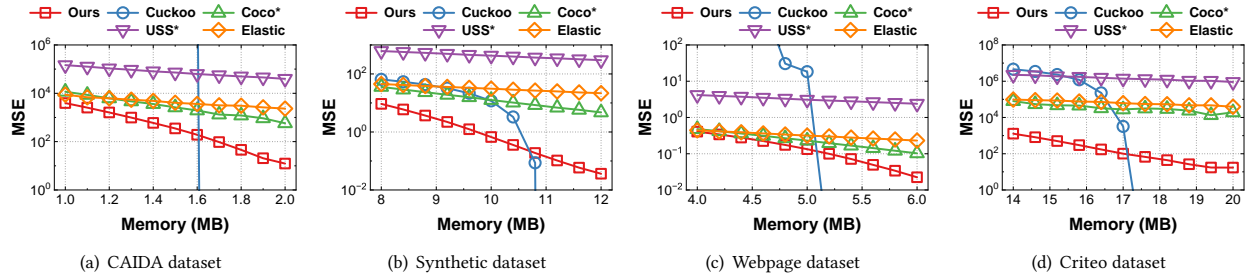


Figure 6: Point Query, MSE.

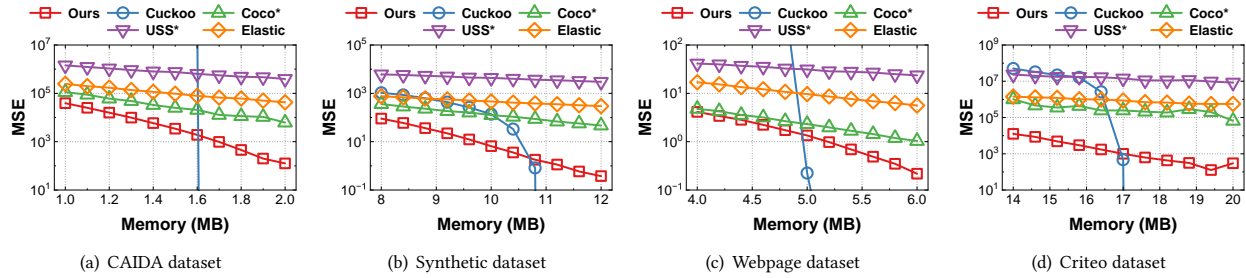


Figure 7: Subset Query, MSE.

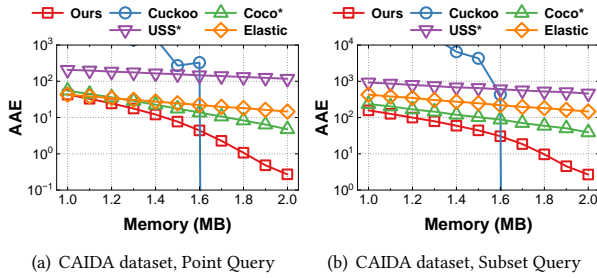


Figure 8: Point Query & Subset Query, AAE.

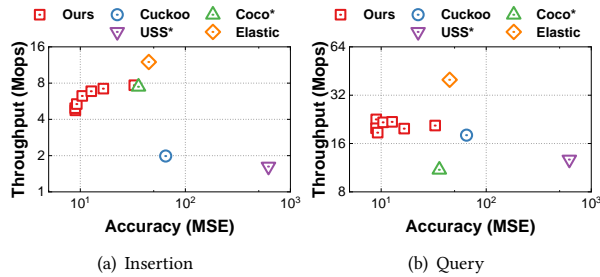


Figure 9: Throughput, Synthetic dataset.

as they cannot be naively adapted to SIM updates. For the synthetic dataset, our default memory setting is 8MB for point and subset queries, and 3MB for Top-K queries.

Statement: Our experimentation encompasses point, subset, and Top-K queries across all datasets, evaluating ARE, AAE, MSE, and recall rates. While the paper presents select results, additional findings are accessible on Github [1], acknowledging space constraints.

6.2 Experiments on Point and Subset Query

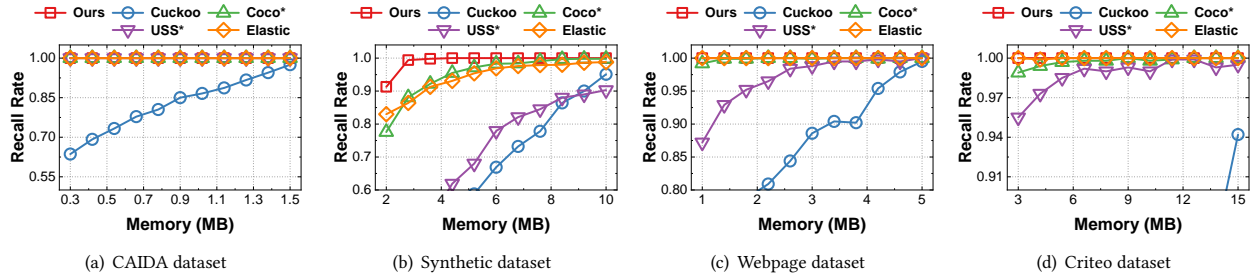
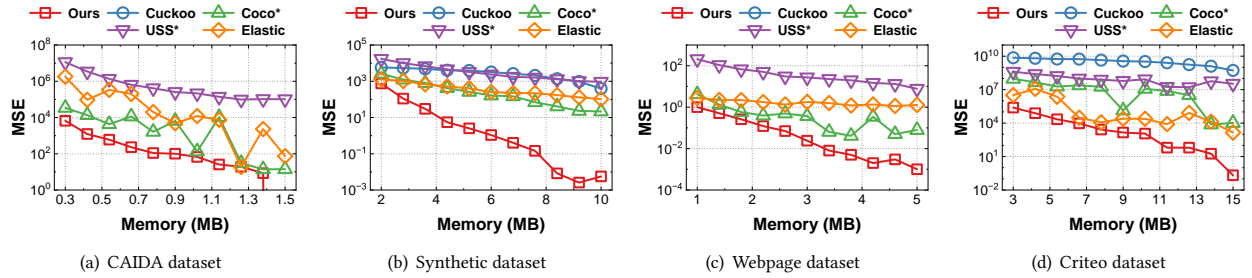
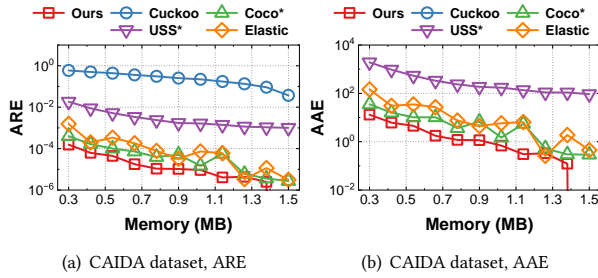
In this section, we vary the memory consumption of different algorithms, evaluating its performance in point and subset query tasks. We ensure that the memory consumption of the comparison algorithms is on par with Carbonyl₄. For different datasets, we allocate memory based on the number of distinct items they contain¹. For point queries, we interrogate all items that have appeared in the data stream; for subset queries, we randomly generate 10,000 sets, each containing 10 items, for our queries. Conclusion draw from other construction methods are similar.

MSE for Point Queries (Figure 6): As depicted in Figures 6(a) to 6(d), within point query tasks, Carbonyl₄ consistently exhibits lower MSE than Coco*, Elastic, and USS*, with reductions of up to 1.11×10^3 -fold compared to Coco* (1.22×10^2 on average), up to 2.69×10^3 -fold compared to Elastic (2.83×10^2 on average), and up to 6.06×10^4 -fold compared to USS* (6.08×10^3 on average). Cuckoo's MSE remains at 0 when the load factor is at or below 94%², due to

¹Synthetic dataset: 898935, CAIDA dataset: 137796, Webpage dataset: 430831, Criteo dataset: 1403213.

²A 94% load factor corresponds different memory sizes across various datasets, specifically, Synthetic dataset: 10.9MB, CAIDA dataset: 1.7MB, Webpage dataset: 5.3MB, Criteo dataset: 17.1MB

fail to insert to accommodate compact memory. We do not compare with counting sketches such as CM [2], Count [4], and SALSA [39],

Figure 10: Top- K Query, Recall rate.Figure 11: Top- K Query, MSE.Figure 12: Top- K Query, ARE & AAE.

its ability to handle a load factor of slightly above 94%. However, as the load factor surpasses 94%, Cuckoo's MSE escalates dramatically, with Carbonyl₄ demonstrating an MSE up to 2.08×10^8 times lower. **AAE for Point Queries (Figure 8):** Figure 8(a) shows that in point query evaluations, Carbonyl₄'s AAE remains below that of Coco*, Elastic, and USS*, potentially offering up to 17.6 times reduction compared to Coco* (5.11 on average), up to 59.1 times to Elastic (11.8 on average), and up to 4.33×10^2 times to USS* (88.1 on average). Once the load factor exceeds 94%, Cuckoo's AAE rises steeply, whereas Carbonyl₄'s AAE is at most 1.63×10^2 times lower. **Throughput for Point Queries (Figure 9):** We set the parameter M of Carbonyl₄ to 0, 1, 2, 4, 10, 20, and 30, respectively, and compare their insertion and query throughput with those of the comparison algorithms. Carbonyl₄'s insertion throughput is higher than that of Cuckoo (1.98Mops) and USS* (1.47Mops), slightly lower than

Coco* (7.46Mops) and Elastic (12.0Mops), and is affected by the parameter M . Specifically, with $M = 30$, Carbonyl₄ will have the highest accuracy and the lowest throughput (4.75Mops); with $M = 0$, the cascading overflow technique will not be used, and Carbonyl₄ will have the lowest accuracy and highest throughput (7.68Mops). With $M = 0$, Carbonyl₄ and Coco* are very similar in terms of accuracy and throughput, because the operations of Carbonyl₄ with $M = 0$ and Coco* are very similar. Given that the accuracy at $M = 10, 20$, and 30 is similar, we recommend using $M = 10$ by default. Carbonyl₄'s query throughput (20.7Mops on average) is higher than Coco* (11.0Mops) and USS* (12.7Mops), similar to Cuckoo (18.0Mops), lower than Elastic (39.9Mops), and is not affected by the parameter M^3 . The query operations of Carbonyl₄ are consistent with those of Cuckoo, thus their throughput is essentially identical. **MSE for Subset Queries (Figure 7):** Illustrated in Figures 6(a) to 6(d), Carbonyl₄'s MSE in subset query tasks always undercuts those of Coco*, Elastic, and USS*, with a diminution of up to 1.57×10^3 -fold compared to Coco* (1.10×10^2 on average), up to 4.39×10^3 -fold compared to Elastic (3.71×10^2 on average), and up to 7.55×10^4 -fold compared to USS* (5.73×10^3 on average). Beyond a 94% load factor, Cuckoo's MSE surges sharply, while Carbonyl₄'s MSE remains up to 2.35×10^8 times lower.

AAE for Subset Queries (Figure 8): As shown in Figure 8(b), for subset query tasks, Carbonyl₄ consistently achieves a lower AAE than Coco*, Elastic, and USS*, with up to 171 times smaller values compared to them (19.5 on average). Cuckoo's AAE increases

³Although there are some differences in query throughput when M varies, we attribute these irregular differences to the randomness of CPU and cache performance.

significantly after the load factor crosses 94%, whereas Carbonyl₄ manages an AAE up to 3.80×10^2 times smaller.

6.3 Experiments on Top-K Query

In this section, we adjust the memory consumption of different algorithms, assessing its accuracy in Top-K query tasks. The memory usage of comparison algorithms is aligned with that of Carbonyl₄. By default, we set $K = 1000$.

Recall for Top-K Queries (Figure 10): Figures 10(a) to 10(d) illustrate that in Top-K query tasks, Carbonyl₄, Coco*, and Elastic maintain the highest recall rates. Conversely, the recall rates for Cuckoo and USS* diminish significantly with increasing load factors. Specifically, on the Synthetic dataset, notable disparities in recall rates among Carbonyl₄, Coco*, and Elastic are observed: Carbonyl₄ attains a recall rate up to 13.7% higher than Coco* (4.07% on average) and up to 13% more than Elastic (4.86% on average). Overall, the recall rate of Carbonyl₄ consistently outperforms and remains near 100%.

MSE for Top-K Queries (Figure 11): As depicted in Figures 11(a) to 11(d), within Top-K query tasks, Carbonyl₄'s MSE invariably falls below that of Coco*, Elastic, USS*, and Cuckoo, with reductions of up to 1.22×10^5 -fold compared to Coco* (6.15×10^3 on average), up to 5.05×10^4 -fold compared to Elastic (2.49×10^3 on average), up to 1.62×10^8 -fold compared to USS* (3.89×10^3 on average), and up to 8.58×10^{11} -fold compared to Cuckoo (6.06×10^{10} on average). The MSE values for Cuckoo are excessively high and are therefore not presented in the Figure 11(a) and 11(c).

AAE & ARE for Top-K Queries (Figure 12): Figures 12(a) and 12(b) show that in Top-K query tasks, the ARE and AAE for Carbonyl₄ are invariably lower than those for Coco*, Elastic, USS*, and Cuckoo, with Carbonyl₄'s ARE and AAE being up to 18.0 times (4.25 on average), up to 21.2 times (8.24×10^2 on average), up to 8.84×10^2 times (2.53×10^2 on average), and up to 8.94×10^5 times (2.52×10^5 on average) smaller than those of Coco*, Elastic, USS*, and Cuckoo, respectively.

6.4 Experiments on Parameters

This section explores the variation in parameters of Carbonyl₄, including maximum search steps M , stop probability p_ϵ , and the number of entries per Balance Bucket d . We evaluate the accuracy and time complexity of Carbonyl₄ for point and Top-K queries and examine the effects of set and increment updates proportions in Synthetic datasets, as well as the skewness of item keys on accuracy.

Accuracy v.s. M and p_ϵ (Figure 13): Figures 13(a) and 13(c) show that in point queries, Carbonyl₄'s AAE declines as M increases, stabilizing when $M \geq 10$. Conversely, AAE rises with increasing p_ϵ , displaying a proportional linear trend. For Figures 13(a) and 13(b), we set $p_\epsilon = 0.1$; For Figures 13(c) and 13(d), we set $M = 100$.

Average Search Steps v.s. M and p_ϵ (Figure 13): Figures 13(b) and 13(d) illustrate that in point queries, Carbonyl₄'s average search steps grow with larger M , indicating a direct linear relationship. As p_ϵ increases, the average search steps decrease inversely, aligning with Theorem 4.

Accuracy v.s. d (Figure 14): Figures 14(a) and 14(b) reveal that Carbonyl₄'s AAE diminishes with higher d , reaching stability for

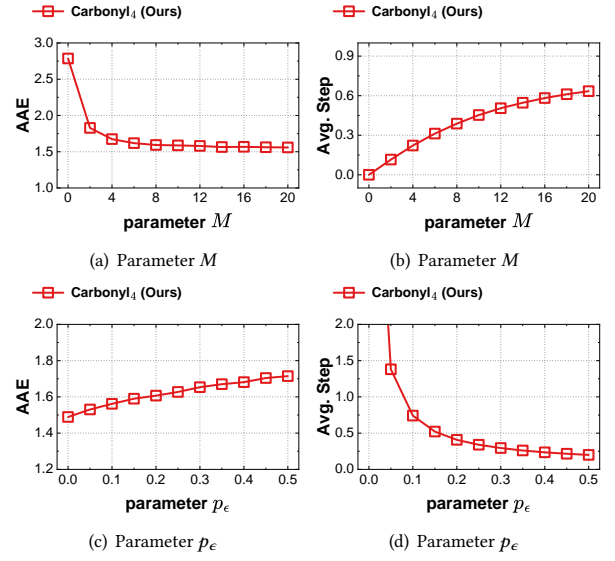


Figure 13: Parameter M & p_ϵ , Synthetic dataset.

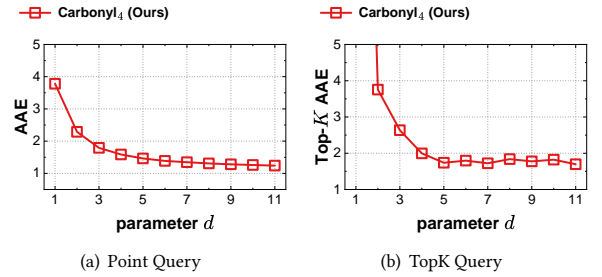


Figure 14: Parameter d , Synthetic dataset.

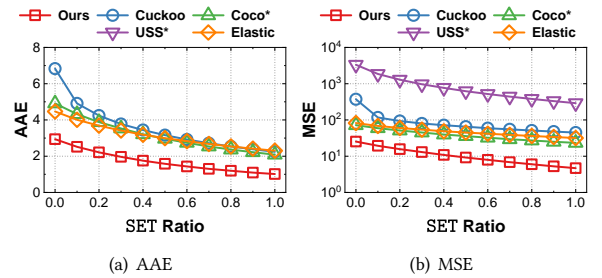


Figure 15: SET Ratio, Synthetic dataset.

$M \geq 6$ in point queries and for $M \geq 4$ in Top-K queries. We recommend $d = 4$ for optimal results.

Accuracy v.s. SET Ratio (Figure 15): Figures 15(a) and 15(b) indicate that on the Synthetic dataset for point queries, all algorithms' AAE and MSE decrease with an increased SET update ratio. Carbonyl₄ shows 2.05, 2.27, 12.0, and 2.80 times lower AAE than

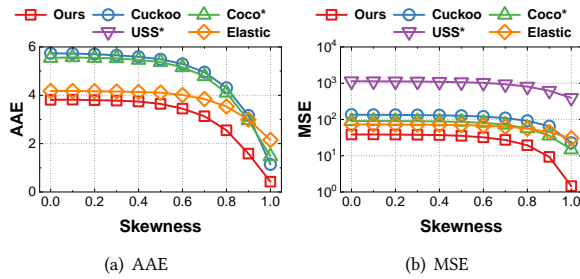


Figure 16: Skewness, Synthetic dataset.

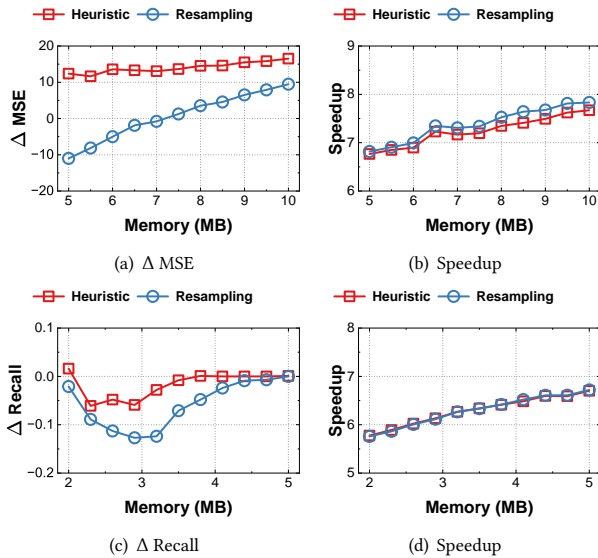


Figure 17: Performance of Shrinking, Synthetic dataset.

Coco*, Elastic, USS*, and Cuckoo respectively; MSE is also 4.98, 6.79, 1.32×10^2 , and 14.7 times lower respectively. This trend confirms that Carbonyl₄'s design is highly effective for mixed set-increment data streams. Taking Elastic as an example, when the SET ratio is 0, Carbonyl₄'s ARE and MSE are respectively 1.52 times and 2.27 times lower than those of Elastic; when the SET ratio is 1, Carbonyl₄'s ARE and MSE are respectively 3.24 times and 6.79 times lower than those of Elastic. This indicates that the cascading overflow technique used by Carbonyl₄ is very effective for SET updates.

Accuracy v.s. Skewness (Figure 16): Figures 15(a) and 15(b) demonstrate that for point queries on the Synthetic dataset, the AAE and MSE for all algorithms decrease with increased data stream skewness. Carbonyl₄ consistently maintains the highest accuracy among all compared algorithms.

6.5 Experiments on Shrinking Algorithm

This section delves into the performance of the re-sampling and heuristic-based shrinking algorithms regarding both accuracy and

speed. We display the difference (Δ) in MSE and recall rate between our proposed two fast shrinking algorithms and the MSE and recall of the shrinking algorithm based on re-building.

Performance of Re-Sampling (Figure 17): Figure 17(a) elucidates the MSE disparities between re-sampling based shrinking and re-building. The MSE of re-sampling is higher than that of re-building when the original Carbonyl₄'s memory consumption exceeds 7MB, while its MSE is lower than re-building when below this memory consumption, attesting to re-sampling's optimality. Figure 17(c) contrasts recall rates, and Figures 17(b) to 17(d) highlight the re-sampling algorithm's velocity, showcasing a 5.76 to 7.83 times acceleration over re-building.

Performance of Heuristic Shrinking (Figure 17): Figure 17(a) compares MSE outcomes between heuristic shrinking and re-building, noting a consistent increase in MSE for the heuristic approach. Figure 17(c) differentiates recall rates, where heuristic shrinking prevails over re-sampling, validating its efficacy in optimizing Top-K queries. Figures 17(b) and 17(d) document the speedup afforded by heuristic shrinking, which achieves a 5.78 to 7.67 hastening compared to re-building.

7 CONCLUSION

In summary, Carbonyl₄ emerges as a robust solution for SIM data streams, bridging the gap where current sketches falter. The algorithm's novel Balance Bucket and Cascading Overflow techniques pave the way for high accuracy and variance optimization, while its memory efficiency is exemplified through innovative shrinking methods. Through rigorous experimentation, Carbonyl₄ has proven to outperform existing algorithms, bolstering its potential as a new standard for data stream analysis. The source codes of Carbonyl₄ are available at GitHub [1].

REFERENCES

- [1] Carbonyl₄. <https://anonymous.4open.science/r/Carbonyl4-C539>.
- [2] Graham Cormode and Shan Muthukrishnan. An improved data stream summary: the count-min sketch and its applications. *Journal of Algorithms*, 55(1):58–75, 2005.
- [3] Cristian Estan and George Varghese. New directions in traffic measurement and accounting: Focusing on the elephants, ignoring the mice. *ACM Transactions on Computer Systems (TOCS)*, 21(3):270–313, 2003.
- [4] Moses Charikar, Kevin Chen, and Martin Farach-Colton. Finding frequent items in data streams. In *International Colloquium on Automata, Languages, and Programming*, pages 693–703. Springer, 2002.
- [5] Yinda Zhang, Zaoying Liu, Ruixin Wang, Tong Yang, Jizhou Li, Ruijie Miao, Peng Liu, Ruwen Zhang, and Junchen Jiang. Cocosketch: High-performance sketch-based measurement over arbitrary partial key query. In *Proceedings of the 2021 ACM SIGCOMM 2021 Conference*, pages 207–222, 2021.
- [6] Daniel Ting. Data sketches for disaggregated subset sum and frequent item estimation. In *Proceedings of the 2018 International Conference on Management of Data*, pages 1129–1140, 2018.
- [7] Ruijie Miao, Yiyao Zhang, Guanyu Qu, Kaicheng Yang, Tong Yang, and Bin Cui. Hyper-uss: Answering subset query over multi-attribute data stream. In *Proceedings of the 29th ACM SIGKDD Conference on Knowledge Discovery and Data Mining*, pages 1698–1709, 2023.
- [8] Ahmed Metwally, Divyakant Agrawal, and Amr El Abbadi. Efficient computation of frequent and top-k elements in data streams. In *International conference on database theory*, pages 398–412. Springer, 2005.
- [9] Tong Yang, Jie Jiang, Peng Liu, Qun Huang, Junzhi Gong, Yang Zhou, Rui Miao, Xiaoming Li, and Steve Uhlig. Elastic sketch: Adaptive and fast network-wide measurements. In *Proceedings of the 2018 Conference of the ACM Special Interest Group on Data Communication*, pages 561–575, 2018.
- [10] Zaoying Liu, Antonis Manousis, Gregory Vorsanger, Vyas Sekar, and Vladimir Braverman. One sketch to rule them all: Rethinking network flow monitoring with univmon. In *Proceedings of the 2016 ACM SIGCOMM Conference*, pages 101–114, 2016.

- [11] Zhewei Wei, Ge Luo, Ke Yi, Xiaoyong Du, and Ji-Rong Wen. Persistent data sketching. In *Proceedings of the 2015 ACM SIGMOD international conference on Management of Data*, pages 795–810, 2015.
- [12] Mimos Garofalakis, Daniel Keren, and Vasilis Samoladas. Sketch-based geometric monitoring of distributed stream queries. *Proceedings of the VLDB Endowment*, 6(10):937–948, 2013.
- [13] Fuheng Zhao, Sujaya Maiyya, Ryan Wiener, Divyakant Agrawal, and Amr El Abbadi. KLL± approximate quantile sketches over dynamic datasets. *Proceedings of the VLDB Endowment*, 14(7):1215–1227, 2021.
- [14] Pinghui Wang, Yiyang Qi, Yuanming Zhang, Qiaozhu Zhai, Chenxu Wang, John CS Lui, and Xiaohong Guan. A memory-efficient sketch method for estimating high similarities in streaming sets. In *Proceedings of the 25th ACM SIGKDD International Conference on Knowledge Discovery & Data Mining*, pages 25–33, 2019.
- [15] Ping Li, Art Owen, and Cun-Hui Zhang. One permutation hashing. *Advances in Neural Information Processing Systems*, 25, 2012.
- [16] Anshumali Shrivastava and Ping Li. Densifying one permutation hashing via rotation for fast near neighbor search. In *International Conference on Machine Learning*, pages 557–565. PMLR, 2014.
- [17] Yikai Zhao, Kaicheng Yang, Zirui Liu, Tong Yang, Li Chen, Shiyi Liu, Naiqian Zheng, Ruixin Wang, Hanbo Wu, Yi Wang, et al. {LightGuardian}: A {full-visibility}, lightweight, in-band telemetry system using sketchlets. In *18th USENIX Symposium on Networked Systems Design and Implementation (NSDI 21)*, pages 991–1010, 2021.
- [18] Hun Namkung, Zaoxing Liu, Daehyeok Kim, Vyas Sekar, and Peter Steenkiste. {SketchLib}: Enabling efficient sketch-based monitoring on programmable switches. In *19th USENIX Symposium on Networked Systems Design and Implementation (NSDI 22)*, pages 743–759, 2022.
- [19] Yuliang Li, Rui Miao, Changhoon Kim, and Minlan Yu. {FlowRadar}: A better {NetFlow} for data centers. In *13th USENIX symposium on networked systems design and implementation (NSDI 16)*, pages 311–324, 2016.
- [20] Michael Mitzenmacher, Rasmus Pagh, and Ninh Pham. Efficient estimation for high similarities using odd sketches. In *Proceedings of the 23rd international conference on World wide web*, pages 109–118, 2014.
- [21] Rasmus Pagh and Flemming Friche Rodler. Cuckoo hashing. *Journal of Algorithms*, 51(2):122–144, 2004.
- [22] Maurice Herlihy, Nir Shavit, and Moran Tzafrir. Hopscotch hashing. In *Distributed Computing: 22nd International Symposium, DISC 2008, Arcachon, France, September 22–24, 2008. Proceedings 22*, pages 350–364. Springer, 2008.
- [23] Jian Kang, Bin Hao, Yuelong Su, Yitao Zhao, Xianfeng Yan, and Shuanghui Hao. A multifunctional encoder with absolute and incremental angle outputs. *IEEE Sensors Journal*, 2023.
- [24] Shi Buhai and Tian Shipeng. A transmission algorithm applicable to incremental and absolute encoder and its implementation. In *2017 2nd International Conference on Advanced Robotics and Mechatronics (ICARM)*, pages 299–304. IEEE, 2017.
- [25] Tamás Lévai, Felicián Németh, Barath Raghavan, and Gabor Retvari. Batchy: batch-scheduling data flow graphs with service-level objectives. In *17th USENIX Symposium on Networked Systems Design and Implementation (NSDI 20)*, pages 633–649, 2020.
- [26] Peiqing Chen, Dong Chen, Lingxiao Zheng, Jizhou Li, and Tong Yang. Out of many we are one: Measuring item batch with clock-sketch. In *Proceedings of the 2021 International Conference on Management of Data*, pages 261–273, 2021.
- [27] Jonathan Perry, Hari Balakrishnan, and Devavrat Shah. Flowtune: Flowlet control for datacenter networks. In *14th USENIX Symposium on Networked Systems Design and Implementation (NSDI 17)*, pages 421–435, 2017.
- [28] The lldb debugger. <https://lldb.lvm.org/>.
- [29] Introduction to jprofiler. <https://www.ej-technologies.com/resources/jprofiler/help/doc/main/introduction.html>.
- [30] Peng Jia, Pinghui Wang, Junzhou Zhao, Ye Yuan, Jing Tao, and Xiaohong Guan. Loglog filter: Filtering cold items within a large range over high speed data streams. In *2021 IEEE 37th International Conference on Data Engineering (ICDE)*, pages 804–815. IEEE, 2021.
- [31] Xun Song, Jiaqi Zheng, Hao Qian, Shiju Zhao, Hongxuan Zhang, Xuntao Pan, and Guihai Chen. Couper: Memory-efficient cardinality estimation under unbalanced distribution. In *2023 IEEE 39th International Conference on Data Engineering (ICDE)*, pages 2753–2765. IEEE, 2023.
- [32] Nikos R Katsipoulakis, Alexandros Labrinidis, and Panos K Chrysanthos. Spear: Expediting stream processing with accuracy guarantees. In *2020 IEEE 36th International Conference on Data Engineering (ICDE)*, pages 1105–1116. IEEE, 2020.
- [33] Sara Farazi and Davood Rafiei. Top-k frequent term queries on streaming data. In *2019 IEEE 35th International Conference on Data Engineering (ICDE)*, pages 1582–1585. IEEE, 2019.
- [34] Siqiang Luo, Subarna Chatterjee, Rafael Ketsetsidis, Niv Dayan, Wilson Qin, and Stratos Idreos. Rosetta: A robust space-time optimized range filter for key-value stores. In *Proceedings of the 2020 ACM SIGMOD International Conference on Management of Data*, pages 2071–2086, 2020.
- [35] Siyuan Sheng, Qun Huang, Sa Wang, and Yungang Bao. Pr-sketch: monitoring per-key aggregation of streaming data with nearly full accuracy. *Proceedings of the VLDB Endowment*, 14(10):1783–1796, 2021.
- [36] Yesdaulet Izenov, Asoke Datta, Florin Rusu, and Jun Hyung Shin. Compass: Online sketch-based query optimization for in-memory databases. In *Proceedings of the 2021 International Conference on Management of Data*, pages 804–816, 2021.
- [37] Fan Deng and Davood Rafiei. New estimation algorithms for streaming data: Count-min can do more. *Webdocs. Cs. Ualberta. Ca*, 2007.
- [38] Tao Li, Shigang Chen, and Yibei Ling. Per-flow traffic measurement through randomized counter sharing. *IEEE/ACM Transactions on Networking*, 20(5):1622–1634, 2012.
- [39] Ran Ben Basat, Gil Einziger, Michael Mitzenmacher, and Shay Vargaftik. Salsa: self-adjusting lean streaming analytics. In *2021 IEEE 37th International Conference on Data Engineering (ICDE)*, pages 864–875. IEEE, 2021.
- [40] Yikai Zhao, Yubo Zhang, Pu Yi, Tong Yang, Bin Cui, and Steve Uhlig. The stair sketch: Bringing more clarity to memorize recent events. In *2022 IEEE 38th International Conference on Data Engineering (ICDE)*, pages 164–177. IEEE, 2022.
- [41] Anshumali Shrivastava, Arnd Christian König, and Mikhail Bilenko. Time adaptive sketches (ada-sketches) for summarizing data streams. In *Proceedings of the 2016 International Conference on Management of Data*, pages 1417–1432, 2016.
- [42] Fuheng Zhao, Divyakant Agrawal, Amr El Abbadi, and Ahmed Metwally. Spacesaving±: An optimal algorithm for frequency estimation and frequent items in the bounded-deletion model.
- [43] Ran Ben Basat, Gil Einziger, Roy Friedman, and Yaron Kassner. Randomized admission policy for efficient top-k and frequency estimation. In *IEEE INFOCOM 2017-IEEE Conference on Computer Communications*, pages 1–9. IEEE, 2017.
- [44] Jizhou Li, Zikun Li, Yifei Xu, Shiqi Jiang, Tong Yang, Bin Cui, Yafei Dai, and Gong Zhang. Wavingsketch: An unbiased and generic sketch for finding top-k items in data streams. In *Proceedings of the 26th ACM SIGKDD International Conference on Knowledge Discovery & Data Mining*, pages 1574–1584, 2020.
- [45] He Huang, Jiakun Yu, Yang Du, Jia Liu, Haipeng Dai, and Yu-E Sun. Memory-efficient and flexible detection of heavy hitters in high-speed networks. *Proceedings of the ACM on Management of Data*, 1(3):1–24, 2023.
- [46] Bohan Zhao, Xiang Li, Boyu Tian, Zhiyu Mei, and Wenfei Wu. Dhs: Adaptive memory layout organization of sketch slots for fast and accurate data stream processing. In *Proceedings of the 27th ACM SIGKDD Conference on Knowledge Discovery & Data Mining*, pages 2285–2293, 2021.
- [47] Edith Cohen, Nick Duffield, Haim Kaplan, Carsten Lund, and Mikkel Thorup. Stream sampling for variance-optimal estimation of subset sums. In *Proceedings of the twentieth annual ACM-SIAM symposium on Discrete algorithms*, pages 1255–1264. SIAM, 2009.
- [48] HO Hartley and JNK Rao. Sampling with unequal probabilities and without replacement. *The Annals of Mathematical Statistics*, pages 350–374, 1962.
- [49] Anonymized internet traces 2018. https://catalog.caida.org/details/dataset/passive_2018_pcap. Accessed:2022-6-29.
- [50] David MW Powers. Applications and explanations of zipf’s law. In *New methods in language processing and computational natural language learning*, 1998.
- [51] Real-life transactional dataset. <http://fimi.ua.ac.be/data/>.
- [52] The critero 1tb click logs dataset. <https://ailab.criteo.com/download-criteo1tb-click-logs-dataset/>.